Near-unity photoluminescence quantum yield in $CsPbBr_3$ nanocrystal solid-state films via post-synthesis treatment with lead bromide

Francesco Di Stasio,[†,‡] Sotirios Christodoulou,[†,‡] Nengjie Huo,[†] and Gerasimos Konstantatos[*,†,§]

† ICFO-Institut de Ciencies Fotoniques, The Barcelona Institute of Science and Technology, 08860 Castelldefels (Barcelona), Spain § ICREA—Institució Catalana de Recerca i Estudis Avançats, Passeig Lluís Companys 23, 08010 Barcelona, Spain

Supporting Information Placeholder

ABSTRACT: Metal halide perovskite nanocrystals (NCs) possess high photoluminescence (PL) quantum yield (Φ_{PL}) and color tunability. Yet, until now, it has been difficult to maintain the high Φ_{PL} observed in solution in spin-coated films. Here, we report a novel $CsPbBr_3$ NCs room-temperature synthesis based on Cs acetate, which displays near-unity Φ_{PL} in solid-state films upon post-synthetic treatment with lead bromide. The as-synthesized NCs show a Φ_{PL} of 80% in spin-coated films but the post-synthesis treatment further enhances the efficiency >95%. The high Φ_{PL} is further confirmed by the monomolecular decay of the PL (5.8 ns) indicating a nearly complete suppression of non-radiative channels. The obtained films demonstrate high stability in air and require around 3 weeks to decrease to half the initial Φ_{PL} value.

Since the first demonstration of $CsPbX_3$ (where X is Br, Cl or I) nanocrystals (NCs) synthesis in 2015,[1] this class of materials have attracted enormous attention thanks to their interesting properties for optoelectronic applications. Both hybrid organic-inorganic ($CH_3NH_3PbX_3$,[2] $CH(NH_2)_2PbX_3$)[3] and all-inorganic perovskite NCs have been successfully employed in efficient solar cells,[4,5] light-emitting diodes,[6,7] white phosphors,[8,9] photodetectors[10] and lasers.[11,12] The main attractiveness of perovskite NCs is their high photoluminescence (PL) quantum yield (Φ_{PL}), which can

tanor their emission wavelength by selecting the halide in the structure[1] or through anion exchange reactions.[14] Both $CsPbX_3$ NCs and their hybrid organic-inorganic counterpart present high Φ_{PL} in solution. Yet, this quantum yield value is typically not retained in films[15] without leaving excess ligands protecting the NCs surface, thus obtaining oily solids not suited for active optoelectronic devices. Retaining efficiency in film is not trivial, since NCs are not as well passivated as in solution, they are exposed to oxygen, moisture or other ambient contaminants, and close packing can lead to energy-transfer to trap-states and increased self-absorption, a process where photons emitted by a NC are absorbed and re-emitted, one or multiple times, by the other neighboring NCs. The PL quenching in solid state is similar to what observed in chalcogenide NCs based on CdSe and CdSe/CdS core-shell architectures which can show near-unity Φ_{PL} in solution as well.[16–19] To obtain high Φ_{PL} in solid films different venues have been explored, for example the engineering of graded-energy-landscape quasi-2D perovskite film,[20] skipping the preparation of NCs altogether, or the addition of organic materials.[21]

Here, we obtain spin-coated films of $CsPbBr_3$ NCs with Φ_{PL} values approaching unity (>95%), thanks to the combination of a novel synthesis at room temperature, and a post-synthetic treatment with lead bromide. Our synthetic approach employs Cs acetate (CsAc) as a precursor and relatively short ligands based on octanoic acid and octylamine. The as-obtained NCs show Φ_{PL}=80% in spin-coated films. Further enhancement of the PL efficiency is obtained via addition to the pristine solution of $PbBr_2$ (dissolved in a 1:1:1 mixture of butylamine:propionic acid:hexane). Moreover, despite the use of short ligands,[5] we have been able to carry out anion exchange reactions obtaining $CsPbBr_{3-x}I_x$ and $CsPbBr_{3-x}Cl_x$ NCs.

The synthesis of $CsPbBr_3$ NCs is carried out via a single-step injection at room temperature and in air, overriding the traditional synthetic protocols that require inert conditions and high temperatures. Here, we used CsAc dissolved in 1-propanol as Cs precursor instead of the more common Cs^+ $_3$ and a fatty acid[1,4] and degassing.[1,22,23] In line with the synthesis reported by Q. A. Akkerman et al. for $CsPbBr_3$ inks,[4] the reaction is carried out in a 1:2 mixture of 1-propanol and hexane. Injection of the $PbBr_2$ precursor solution ($PbBr_2$ dissolved in a mixture of 1:1:1 1-propanol:octanoic acid:octylamine) into the reaction flask containing Cs^+ induces immediate formation of the NCs, which are then purified via centrifugation and dispersed in toluene. Figure 1a reports a bright-field TEM image of the as-synthesized NCs (an additional TEM image is reported in the supporting information, see Figure S1). The NCs are highly polydispersed with irregular shapes and sizes. From TEM analysis we measured variable lateral sizes of the NCs: from

7x7 up to 31x26 nm (Figure SI1). Importantly, most NCs show an anisotropic shape resembling nanoplatelets.[4] The inter-nanocrystal distance estimated from HRTEM is of 1±0.2 nm thanks to the employment of short ligands during synthesis (inset of Figure 1a). X-ray diffraction patterns (XRD, Figure 1b) show that the crystal structure of the NCs is compatible with both orthorhombic and cubic phases, ruling out the presence of the not-luminescent Cs_4PbBr_6 phase (see figure SI2).[24,25] The presence of only the $CsPbBr_3$ phase is further demonstrated by energy-dispersive x-ray (EDX) measurements, which reveal a 1:1:3 ratio between Cs, Pb and Br, respectively. Initial reports have deemed the cubic structure as the only optically active phase[1] but recent literature have shown that the orthorhombic phase is luminescent as well,[4] and it is the actual structure of inorganic perovskite NCs.[26] Considering these conflicting results, we cannot unambiguously assign the crystal structure phase of the NCs and, a mixture of orthorhombic and cubic NCs cannot be ruled out.

Our synthetic approach induces the formation of $CsPbBr_3$ NCs with a hybrid morphology between inks[4] and nanoplatelets.[22] The use of acetate based precursor combined with longer ligands it is known to give rise to anisotropic NCs, as in the case of CdSe nanoplatelets.[27] Furthermore, $CsPbX_3$ nanoplatelets can be prepared employing polar solvents and the use of alcohols during synthesis does not allow precise shape control.[22] In Figure 1c we show the optical absorption and PL spectra of the $CsPbBr_3$ NCs in solution and in spin-coated films. As-synthesized NCs in solution display a PL centered at 515 nm (full-width-half-maximum, FWHM = 25 nm) and two main absorption peaks at 468 and 449 nm. Considering the large polydispersity of our NCs and the presence of the $CsPbBr_3$ phase only, the main absorption peaks can be associated with the smallest NCs while the emission at 515 nm indicates that the PL arises from NCs with near-bulk dimensions.[28] Spin-coated films from the same solution do not show any significant PL red-shift (the FWHM increases to 30 nm) while the main optical absorption features show a blue shift of ≈ 5 nm, similar to what observed for $CsPbBr_3$ NCs films prepared via centrifugation.[15] Importantly, we measured an increase in Φ_{PL} from 54±5 to 80±8% transferring the NCs from solution to film. The enhancement is surprising, as one would expect a lower Φ_{PL} in film as discussed in the introduction. Yet, $CsPbBr_3$ NCs possess an intrinsic defect-tolerant structure[2,29] strongly reducing the effect of traps on the PL. Furthermore, the large spectral spacing of 47 nm (0.24 eV) between the main absorption features and the PL induces a limited self-absorption in dense NC films.

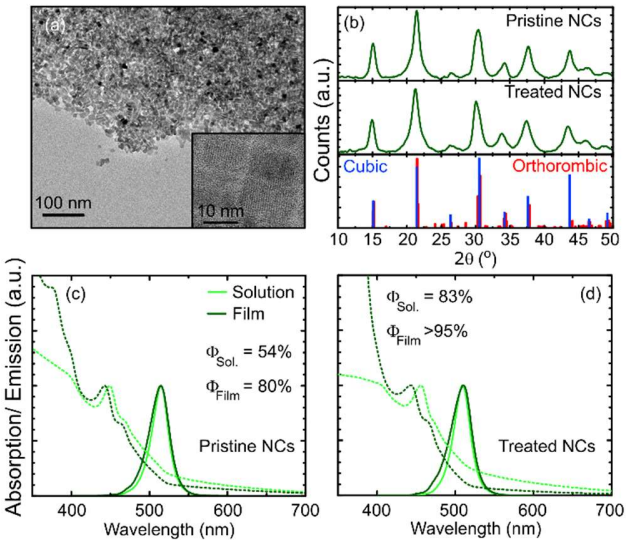

Figure 1. (a) TEM image of the as-synthesized $CsPbBr_3$ NCs and (inset) high-resolution TEM of the NCs. (b) X-ray diffraction pattern collected from a NC spin-coated film before and after treatment in solution. The red bars represent the diffraction pattern for orthorhombic $CsPbBr_3$ (ICSD 97851) while the blue bars are the pattern for cubic $CsPbBr_3$ (ICSD 97852). Optical absorption (dashed lines) and steady-state PL (solid lines) spectra of $CsPbBr_3$ NCs in toluene solution and spin-coated film before (c) and after treatment (d).

The increase in Φ_{PL} can be explained tentatively by the removal of impurities still present in solution after synthesis. Polar species such as 1-propanol or Cs^+ used in the reaction can cause ligand desorption from the NCs surface.[30] In our synthetic approach the obtained NCs were purified only once via centrifugation, as additional steps or addition of an antisolvent (for example, methyl acetate) have a detrimental effect on the Φ_{PL}. Upon spin-coating, it is possible that impurities are washed away. This hypothesis is supported by the lower Φ_{PL} of 45±5% measured in drop-cast films where impurities are left and solvent can be trapped inside. Nevertheless, self-absorption depends on the film thickness, thus it can generate the discrepancy in Φ_{PL} between drop-cast and spin-coated films. Furthermore, a variety of effects can cause the observed PL enhancement as, for example, variation in the dielectric constant of the surrounding medium (from toluene solution to air) and the way NCs are packed in the film.

As reported, by J. De Roo et al.,[30] high amine content in solution induces a stronger binding of the carboxylic acid on the NCs surface thus enhancing the PL efficiency. Similarly, Z. Wei et al.[31] have shown that $CsPbBr_3$ films treated with CsBr display enhanced Φ_{PL}. For these reasons, we have investigated post-synthesis treatment of our $CsPbBr_3$ NCs based on the addition of small amounts of amines, carboxylic acids and reaction precursors/complexes (0.6% v/v for a typical synthesis). We have focused on small carboxylic acids and amines since one of the main advantage of our NCs is the formation of dry films without the need of complex procedures that can be detrimental for the PL efficiency. Addition of only a small amount of carboxylic acids to the pristine $CsPbBr_3$ NCs toluene solution induces a drop in Φ_{PL} (see Table SI1 for a summary of the post-synthesis treatment

results) with the solution turning from green to yellow. This effect is observed by adding acids with a short carbon chain, from propionic to hexanoic. Addition of carboxylic acids with longer chains, such as oleic acid, does not modify the PL properties of the NCs. It is possible that the higher acidity of small carboxylic acids interfere with the acid/base equilibrium at the NCs surface, causing once again ligand desorption.[30] Similarly, sole introduction of CsAc/1-propanol precursor turns the NC solution white and completely quenches the photoluminescence in few seconds. On the contrary, adding 0.6% (v/v) butylamine enhances further the PL of the NCs. Further amine addition causes cleavage of the NCs into smaller ones (as demonstrated by the appearance of blue-shifted PL peaks, see Figure SI3) and it turns the solution white in few hours, suggesting NCs decomposition.[24,30] Finally, introducing $PbBr_2$ in combination with propionic acid and butylamine into the NC solution, both enhances Φ_{PL} and it stabilizes the NCs. Figure 1d shows the PL and absorption spectra of the NCs in solution and in film after treatment with $PbBr_2$. The PL spectrum is blue-shifted of 5 nm (510 nm) compared to the pristine sample and a red-shift of the main absorption peaks is observed (475 and 456 nm). A PL blue-shift has been reported for $CsPbBr_3$ powders treated with CsBr[31] and it has been assigned to the presence of excess Br. In our case, excess of Br is present due to the introduction of $PbBr_2$ but the same PL blue-shift is observed upon addition of only butylamine (see Figure SI3). On the other hand, the red-shift of the main absorption features indicates an increase in size of the NCs upon addition of $PbBr_2$. This interpretation is further supported by TEM images collected from the treated sample and their analysis (see Figure SI4) where the average width and length of the NCs is increased by 14±2%. Importantly, the XRD spectrum (Figure 1b) do not reveal any difference in crystal structure after treatment. These changes in PL properties are followed by an increase in Φ_{PL} from 54±5% to 83±8%. Spin-coated films from treated NCs show the same PL as observed in solution while the Φ_{PL} approaches 100%. The observed near-unity PL efficiency in films is remarkable and to our knowledge, it has never been observed in NC films. Nevertheless, another important parameter to take into account is the NCs stability. Pristine NC solutions stored at 4 °C turn yellow and barely luminescent after 48 hours. The treatment enhances the stability, with the solution maintaining its original PL properties for over 2 months upon storage in dark and at low temperature. Similarly, films spin-coated from pristine solutions reach half the initial Φ_{PL} after one week of storage in air, while films from treated solutions need 3 weeks to reach half the efficiency value.

Time-resolved PL measurements carried out in solutions and films show an overall suppression of non-radiative components of the NC PL decay upon post-synthesis treatment and spin-coating. The most striking effect is observed in solution where the average PL lifetime increases from 2.1 to 4.7 ns (Figure 2a) upon $PbBr_2$ treatment thanks to a reduction in the initial sub-ns decay component (see Table 1 for a summary of the fitting parameters). The suppression of the fast component followed by the increase in Φ_{PL} identifies this channel as a PL quenching mechanism that is mitigated by the post-synthesis treatment. Nonetheless, the PL decay in solution remains multi-exponential indicating a complex de-excitation pathway which is not observed in $CsPbBr_3$ NC solutions displaying near-unity Φ_{PL}.[13] Upon spin-coating of the pristine NCs (Figure 2b), the PL decay becomes nearly mono-molecular, with only a 7% contribution of the long-lived lifetime component assigned to charge-trapping (see Table 1). The long-lived component is further reduced to 2% of the overall PL decay by using the treated NC solution for film preparation. Importantly, comparing the pristine films to the treated ones, a secondary effect is observed: the dominant decay channel is shortened from 9.6 (pristine film) to 5.8 ns (treated film). Considering the increase in Φ_{PL} from 83% to >95%, the shortening of the dominant PL decay channel indicates an increase in the radiative-rate induced by faster exciton recombination in the NCs. Power dependent measurements reveal near-unity Φ_{PL} in film pumping up to 30 mW/cm² (Figure 2c). At low excitation density we do not observe a drop in efficiency indicating that exciton recombination is not trap-limited.[22] Above 30 mW/cm², multi-exciton effects as Auger-recombination can be detrimental for the PL efficiency,[32] and sample degradation can take place.

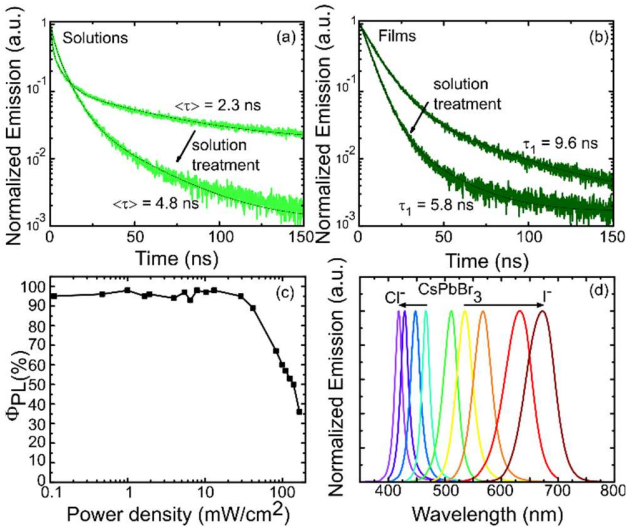

Figure 2. Time-resolved PL measured at the PL peak (λ = 515-510 nm) for the $CsPbBr_3$ NCs in toluene solution (a) and from a spin-coated film (b). The intensity average lifetime in (a) ($<\tau>$) has been calculated as following: $<\tau>=(I_1\tau_1+I_2\tau_2)/(I_1+I_2)$, hence excluding the long lifetime component τ_3 . (c) Photoluminescence efficiency (Φ_{PL}) Vs excitation power density (λ_{exc} = 405 nm) for a spin-coated film from treated NCs. (d) PL spectra recorded from a $CsPbBr_3$ NC solution and anion exchanged samples with Cl^- ($CsPbBr_{3-x}Cl_x$) or I^- ($CsPbBr_{3-x}I_x$).

The observed near-unity Φ_{PL} in film originates from a combination of effects. First, our synthetic method produces $CsPbBr_3$ NCs showing a high Φ_{PL} of 80% in spin-coated films. Until now, many of the reported synthetic procedures have shown lower Φ_{PL} in films. For example, $CsPbBr_3$ NCs inks prepared with a similar procedure possess a PL efficiency around 35%.[4] Other examples are $CsPbBr_3$ NCs prepared with longer ligands such as oleic acid,[1] or nanoplatelets.[22] As previously introduced, the high PL efficiency observed in our NCs films can partially be assigned to the large spectral spacing between the main absorption features and the PL peak which reduces self-absorption in the film.

Table 1. Summary of the parameters used for fitting the PL decays of $CsPbBr_3$ NCs in solution and in spin-coated films. The

PL decay fitting was carried out with a three-exponential function $(I = I_0 + I_1 e^{(-t/\tau_1)} + I_2 e^{(-t/\tau_2)} + I_3 e^{(-t/\tau_3)})$ *for solutions and a two-exponential one* $(I = I_0 + I_1 e^{(-t/\tau_1)} + I_2 e^{(-t/\tau_2)})$ *for spin-coated films.*

	I_1	τ_1 (ns)	I_2	τ_2 (ns)	I_3	τ_3 (ns)	Φ_{PL} (%)
pristine solution	0.64	0.87	0.27	5.8	0.09	50	54
treated solution	0.43	2.04	0.52	7.1	0.05	29.6	80
pristine film	0.93	9.57	0.07	42			83
treated film	0.98	5.8	0.02	23			>95

Another beneficial impact is given by the addition of the $PbBr_2$ solution which induces a stronger ligand binding[30] at the NCs surface and it introduces a Br excess,[31] both beneficial effects for the PL efficiency. It has been demonstrated that exposure of $CsPbBr_3$ NCs films to butylamine induces the formation of the not-luminescent oD Cs_4PbBr_6 phase.[33] In our case we observe a similar phenomenon as the treatment is very sensitive to the amount of butylamine added. Nonetheless, judiciously adding the $PbBr_2$ solution maintains the beneficial effect of the amine treatment but eliminates the need to control precisely the volume added (as addition of more than 0.6% v/v of butylamine degrades the NCs, see Table SI1). Importantly, while this paper was under revision, J. Y. Woo, et al.[34] reported an increased Φ_{PL} and stability via surface passivation of $CsPbBr_3$ NCs by adding $ZnBr_2$ into the reaction flask. We cannot rule out that a similar mechanism is at play in our post-synthesis treatment.[34] The aforementioned effects combine with the PL enhancement observed after spin-coating.

An important advantage of perovskite NCs is the possibility to carry out anion-exchange reaction, thus changing their emission color.[3,14,35] For this reason, we have investigated anion-exchange reactions on our NCs using Cl^- or I^- anions (see methods in the supporting information). Figure 2d reports the PL spectra of the anion exchanged NCs in toluene solutions. The reactions were carried out by quickly injecting different amounts of a PbI_2 or $PbCl_2$ solutions (in 1:1:1 mixture of octanoic acid:octylamine:hexane) in a diluted treated $CsPbBr_3$ NC solution. The anion-exchange takes place within seconds with the solution changing color (see photo in Figure SI5). The PL can be spectrally tuned between 418 and 673 nm. The high Φ_{PL} observed in treated $CsPbBr_3$ NC solutions (83±8%) is partially maintained in the exchanged samples, with $CsPbBr_{3-x}I_x$ displaying Φ_{PL} = 50±5% and $CsPbBr_{3-x}Cl_x$ achieving Φ_{PL} = 25±5% on average (see Table SI2 for the Φ_{PL} values, PL peak position and PL FWHM and Figure SI5 for a photo of the solutions).

In conclusion, we have demonstrated a room temperature synthesis of $CsPbBr_3$ NCs that can be carried out in air. Post-synthesis treatment of the NCs induces an enhancement of the photoluminescence efficiency. Importantly, films fabricated from the $CsPbBr_3$ NCs demonstrate near-unity photoluminescence efficiency, which arises from a combination of the synthetic method employed and PL enhancement through treatment with $PbBr_2$. We believe the synthetic approach here proposed can be employed for the fabrication of a variety of optoelectronic devices where high photoluminescence efficiency is needed (e.g. light-emitting diodes).

ASSOCIATED CONTENT

Supporting Information

The Supporting Information is available free of charge on the ACS Publications website. Experimental methods, TEM images of pristine and treated $CsPbBr_3$ NCs, additional XRD data, table with a summary of the different treatments and additional optical characterization data are included

AUTHOR INFORMATION

Corresponding Author

*gerasimos.konstantatos@icfo.eu

Author Contributions

‡F. Di Stasio and S. Christodoulou contributed equally to this work

Notes

The authors declare no competing financial interests.

ACKNOWLEDGMENT

The authors acknowledge financial support from the European Research Council (ERC) under the European Union's Horizon 2020 research and innovation programme (grant agreement no. 725165), the Spanish Ministry of Economy and Competitiveness (MINECO), and the "Fondo Europeo de Desarrollo Regional" (FEDER) through grant MAT2014-56210-R. The authors also acknowledge financial support from Fundacio Privada Cellex, the program CERCA and from the Spanish Ministry of Economy and Competitiveness, through the "Severo Ochoa" Programme for Centres of Excellence in R&D (SEV-2015-0522). F. Di Stasio and S. Christodoulou acknowledge support from two Marie Curie Standard European Fellowships ("NANOPTO", H2020-MSCA-IF-2015-703018 and "NAROBAND", H2020-MSCA-IF-2016-750600).

REFERENCES

(1) Protesescu, L.; Yakunin, S.; Bodnarchuk, M. I.; Krieg, F.; Caputo, R.; Hendon, C. H.; Yang, R. X.; Walsh, A.; Kovalenko, M. V. Nanocrystals of Cesium Lead Halide Perovskites (CsPbX3, X = Cl, Br, and I): Novel Optoelectronic Materials Showing Bright Emission with Wide Color Gamut. *Nano Lett.* **2015**, *15* (6), 3692–3696.

(2) Dirin, D. N.; Protesescu, L.; Trummer, D.; Kochetygov, I. V; Yakunin, S.; Krumeich, F.; Stadie, N. P.; Kovalenko, M. V. Harnessing Defect-Tolerance at the Nanoscale: Highly Luminescent Lead Halide Perovskite Nanocrystals in Mesoporous Silica Matrixes. *Nano Lett.* **2016**, *16* (9), 5866–5874.

(3) Levchuk, I.; Osvet, A.; Tang, X.; Brandl, M.; Perea, J. D.; Hoegl, F.; Matt, G. J.; Hock, R.; Batentschuk, M.; Brabec, C. J. Brightly Luminescent and Color-Tunable Formamidinium Lead Halide Perovskite FAPbX3 (X = Cl, Br, I) Colloidal Nanocrystals. *Nano Lett.* **2017**, *17* (5), 2765–2770.

(4) Akkerman, Q. A.; Gandini, M.; Di Stasio, F.; Rastogi, P.; Palazon, F.; Bertoni, G.; Ball, J. M.; Prato, M.; Petrozza, A.; Manna, L. Strongly Emissive Perovskite Nanocrystal Inks for High-Voltage Solar Cells. *Nat. Energy* **2016**, *2*, 16194.

(5) Swarnkar, A.; Marshall, A. R.; Sanehira, E. M.; Chernomordik, B. D.; Moore, D. T.; Christians, J. A.; Chakrabarti, T.; Luther, J. M. Quantum Dot–induced Phase Stabilization of α-$CsPbI_3$ Perovskite for High-Efficiency Photovoltaics. *Science* **2016**, *354* (6308), 92-95.

(6) Li, J.; Xu, L.; Wang, T.; Song, J.; Chen, J.; Xue, J.; Dong, Y.; Cai, B.; Shan, Q.; Han, B.; Zeng, H. 50-Fold EQE Improvement up to 6.27% of Solution-Processed All-Inorganic Perovskite CsPbBr 3 QLEDs via Surface Ligand Density Control. *Adv. Mater.* **2017**, *29* (5), 1603885.

(7) Li, G.; Rivarola, F. W. R.; Davis, N. J. L. K.; Bai, S.; Jellicoe, T. C.; de la Peña, F.; Hou, S.; Ducati, C.; Gao, F.; Friend, R. H.; Greenham, N. C.; Tan, Z.-K. Highly Efficient Perovskite Nanocrystal Light-Emitting Diodes Enabled by a Universal Crosslinking Method. *Adv. Mater.* **2016**, *28* (18), 3528–3534.

(8) Palazon, F.; Di Stasio, F.; Akkerman, Q. A.; Krahne, R.; Prato, M.; Manna, L. Polymer-Free Films of Inorganic Halide Perovskite Nanocrystals as UV-to-White Color-Conversion Layers in LEDs. *Chem. Mater.* **2016**, *28* (9), 2902–2906.

(9) Pathak, S.; Sakai, N.; Wisnivesky Rocca Rivarola, F.; Stranks, S. D.; Liu, J.; Eperon, G. E.; Ducati, C.; Wojciechowski, K.; Griffiths, J. T.; Haghighirad, A. A.; Pellaroque, A.; Friend, R. H.; Snaith, H. J. Perovskite Crystals for Tunable White Light Emission. *Chem. Mater.* **2015**, *27* (23), 8066–8075.

(10) Kwak, D.-H.; Lim, D.-H.; Ra, H.-S.; Ramasamy, P.; Lee, J.-S. High Performance Hybrid Graphene-CsPbBr3-xIx Perovskite Nanocrystal Photodetector. *RSC Adv.* **2016**, *6* (69), 65252–65256.

(11) Yakunin, S.; Protesescu, L.; Krieg, F.; Bodnarchuk, M. I.; Nedelcu, G.; Humer, M.; De Luca, G.; Fiebig, M.; Heiss, W.; Kovalenko, M. V. Low-Threshold Amplified Spontaneous Emission and Lasing from Colloidal Nanocrystals of Caesium Lead Halide Perovskites. *Nat. Commun.* **2015**, *6*, 8056.

(12) Protesescu, L.; Yakunin, S.; Kumar, S.; Bär, J.; Bertolotti, F.; Masciocchi, N.; Guagliardi, A.; Grotevent, M.; Shorubalko, I.; Bodnarchuk, M. I.; Shih, C.-J.; Kovalenko, M. V. Dismantling the "Red Wall" of Colloidal Perovskites: Highly Luminescent Formamidinium and Formamidinium–Cesium Lead Iodide Nanocrystals. *ACS Nano* **2017**, *11* (3), 3119–3134.

(13) Koscher, B. A.; Swabeck, J. K.; Bronstein, N. D.; Alivisatos, A. P. Essentially Trap-Free CsPbBr3 Colloidal Nanocrystals by Postsynthetic Thiocyanate Surface Treatment. *J. Am. Chem. Soc.* **2017**, *139* (19), 6566–6569.

(14) Akkerman, Q. A.; D'Innocenzo, V.; Accornero, S.; Scarpellini, A.; Petrozza, A.; Prato, M.; Manna, L. Tuning the Optical Properties of Cesium Lead Halide Perovskite Nanocrystals by Anion Exchange Reactions. *J. Am. Chem. Soc.* **2015**, *137* (32), 10276–10281.

(15) Kim, Y.; Yassitepe, E.; Voznyy, O.; Comin, R.; Walters, G.; Gong, X.; Kanjanaboos, P.; Nogueira, A. F.; Sargent, E. H. Efficient Luminescence from Perovskite Quantum Dot Solids. *ACS Appl. Mater. Interfaces* **2015**, *7* (45), 25007–25013.

(16) Gao, Y.; Peng, X. Photogenerated Excitons in Plain Core CdSe Nanocrystals with Unity Radiative Decay in Single Channel: The Effects of Surface and Ligands. *J. Am. Chem. Soc.* **2015**, *137* (12), 4230–4235.

(17) Greytak, A. B.; Allen, P. M.; Liu, W.; Zhao, J.; Young, E. R.; Popovic, Z.; Walker, B. J.; Nocera, D. G.; Bawendi, M. G. Alternating Layer Addition Approach to CdSe/CdS Core/shell Quantum Dots with near-Unity Quantum Yield and High on-Time Fractions. *Chem. Sci.* **2012**, *3* (6), 2028–2034.

(18) Coropceanu, I.; Rossinelli, A.; Caram, J. R.; Freyria, F. S.; Bawendi, M. G. Slow-Injection Growth of Seeded CdSe/CdS Nanorods with Unity Fluorescence Quantum Yield and Complete Shell to Core Energy Transfer. *ACS Nano* **2016**, *10* (3), 3295–3301.

(19) Dai, X.; Zhang, Z.; Jin, Y.; Niu, Y.; Cao, H.; Liang, X.; Chen, L.; Wang, J.; Peng, X. Solution-Processed, High-Performance Light-Emitting Diodes Based on Quantum Dots. *Nature* **2014**, *515* (7525), 96–99.

(20) Quan, L. N.; Zhao, Y.; García de Arquer, F. P.; Sabatini, R.; Walters, G.; Voznyy, O.; Comin, R.; Li, Y.; Fan, J. Z.; Tan, H.; Pan, J.; Yuan, M.; Bakr, O. M.; Lu, Z.; Kim, D. H.; Sargent, E. H. Tailoring the Energy Landscape in Quasi-2D Halide Perovskites Enables Efficient Green-Light Emission. *Nano Lett.* **2017**, *17* (6), 3701–3709.

(21) Zhang, X.; Sun, C.; Zhang, Y.; Wu, H.; Ji, C.; Chuai, Y.; Wang, P.; Wen, S.; Zhang, C.; Yu, W. W. Bright Perovskite Nanocrystal Films for Efficient Light-Emitting Devices. *J. Phys. Chem. Lett.* **2016**, *7* (22), 4602–4610.

(22) Akkerman, Q. A.; Motti, S. G.; Srimath Kandada, A. R.; Mosconi, E.; D'Innocenzo, V.; Bertoni, G.; Marras, S.; Kamino, B. A.; Miranda, L.; De Angelis, F.; Petrozza, A.; Prato, M.; Manna, L. Solution Synthesis Approach to Colloidal Cesium Lead Halide Perovskite Nanoplatelets with Monolayer-Level Thickness Control. *J. Am. Chem. Soc.* **2016**, *138* (3), 1010–1016.

(23) Sun, S.; Yuan, D.; Xu, Y.; Wang, A.; Deng, Z. Ligand-Mediated Synthesis of Shape-Controlled Cesium Lead Halide Perovskite Nanocrystals via Reprecipitation Process at Room Temperature. *ACS Nano* **2016**, *10* (3), 3648–3657.

(24) Palazon, F.; Dogan, S.; Marras, S.; Locardi, F.; Nelli, I.; Rastogi, P.; Ferretti, M.; Prato, M.; Krahne, R.; Manna, L. From CsPbBr3 Nano-Inks to Sintered CsPbBr3–CsPb2Br5 Films via Thermal Annealing: Implications on Optoelectronic Properties. *J. Phys. Chem. C* **2017**, *121* (21), 11956–11961.

(25) Akkerman, Q. A.; Park, S.; Radicchi, E.; Nunzi, F.; Mosconi, E.; De Angelis, F.; Brescia, R.; Rastogi, P.; Prato, M.; Manna, L. Nearly Monodisperse Insulator Cs4PbX6 (X = Cl, Br, I) Nanocrystals, Their Mixed Halide Compositions, and Their Transformation into CsPbX3 Nanocrystals. *Nano Lett.* **2017**, *17* (3), 1924–1930.

(26) Cottingham, P.; Brutchey, R. L. On the Crystal Structure of Colloidally Prepared CsPbBr3 Quantum Dots. *Chem. Commun.* **2016**, *52* (30), 5246–5249.

(27) Grim, J. Q.; Christodoulou, S.; Di Stasio, F.; Krahne, R.; Cingolani, R.; Manna, L.; Moreels, I. Continuous-Wave Biexciton Lasing at Room Temperature Using Solution-Processed Quantum Wells. *Nat. Nanotechnol.* **2014**, *9* (11), 891–895.

(28) Brennan, M. C.; Zinna, J.; Kuno, M. Existence of a Size-Dependent Stokes Shift in CsPbBr3 Perovskite Nanocrystals. *ACS Energy Lett.* **2017**, 1487–1488.

(29) Kang, J.; Wang, L.-W. High Defect Tolerance in Lead Halide Perovskite CsPbBr3. *J. Phys. Chem. Lett.* **2017**, *8* (2), 489–493.

(30) De Roo, J.; Ibáñez, M.; Geiregat, P.; Nedelcu, G.; Walravens, W.; Maes, J.; Martins, J. C.; Van Driessche, I.; Kovalenko, M. V; Hens, Z. Highly Dynamic Ligand Binding and Light Absorption Coefficient of Cesium Lead Bromide Perovskite Nanocrystals. *ACS Nano* **2016**, *10* (2), 2071–2081.

(31) Wei, Z.; Perumal, A.; Su, R.; Sushant, S.; Xing, J.; Zhang, Q.; Tan, S. T.; Demir, H. V.; Xiong, Q. Solution-Processed Highly Bright and Durable Cesium Lead Halide Perovskite Light-Emitting Diodes. *Nanoscale* **2016**, *8* (42), 18021–18026.

(32) Makarov, N. S.; Guo, S.; Isaienko, O.; Liu, W.; Robel, I.; Klimov, V. I. Spectral and Dynamical Properties of Single Excitons, Biexcitons, and Trions in Cesium–Lead-Halide Perovskite Quantum Dots. *Nano Lett.* **2016**, *16* (4), 2349–2362.

(33) Palazon, F.; Almeida, G.; Akkerman, Q. A.; De Trizio, L.; Dang, Z.; Prato, M.; Manna, L. Changing the Dimensionality of Cesium Lead Bromide Nanocrystals by Reversible Postsynthesis Transformations with Amines. *Chem. Mater.* **2017**, *29* (10), 4167–4171.

(34)Woo J. Y., Kim Y., Bae J., Kim T. G., Kim J. W., Lee D. C.· Jeong S. Highly Stable Cesium Lead Halide Perovskite Nanocrystals through in Situ Lead Halide Inorganic Passivation *Chem. Mater.* **2017** DOI: 10.1021/acs.chemmater.7b02669

(35) Nedelcu, G.; Protesescu, L.; Yakunin, S.; Bodnarchuk, M. I.; Grotevent, M. J.; Kovalenko, M. V. Fast Anion-Exchange in Highly Luminescent Nanocrystals of Cesium Lead Halide Perovskites (CsPbX3, X = Cl, Br, I). *Nano Lett.* **2015**, *15* (8), 5635–5640.

Table of Contents artwork